FARADAY

Adsorption and photochemistry of ethene on NaCl crystallites

Kyle Willian,† Otto Berg‡ and George E. Ewing*
Department of Chemistry, Indiana University, Bloomington, IN 47405, USA

IR spectra, thermodynamics and photochemistry of ethene, C_2H_4, physisorbed onto NaCl(100) cuboids of a sublimed polycrystalline film have been examined. The heat of adsorption of ethene onto the NaCl film ranges $-10 \pm 3 < \Delta_{ads}H < -17 \pm 3$ kJ mol^{-1} over a coverage range of $0.5 < \Theta < 1.0$. The vibrational spectrum of the adsorbed ethene resembles that of condensed phase and matrix isolated ethene where intensities and frequencies are only slightly modified from the gas phase. The ethene, adsorbed at less than a full monolayer on the crystallites, is then subjected to 184.9 nm light whereupon it photodissociates almost exclusively into acetylene and H_2. Further, it is not the ethene molecules, but the NaCl substrate which appears to be the main antenna of photon capture. We present evidence that suggests that the excitation is stored as self-trapped excitons (STEs) in the NaCl. This energy is then passed to the adsorbed ethene *via* triplet–triplet energy transfer. It is proposed that the acetylene is produced either through a triplet ethylidene or vinylidene intermediate.

Professor Norman Sheppard, FRS, has made many original contributions to spectroscopy at interfaces. He was among the first to use alkali halide crystallite surfaces for the IR study of adlayers of hydrogen halides.[1–3] The technique of preparing crystallites of alkali halides, whose surfaces are the platforms for adsorbed molecules, and monitoring their physical and chemical processes by infrared spectroscopy was developed by Kozirovski and Folman.[4] Following the inspiration of these pioneering studies, we offer our photochemical investigation of C_2H_4 on NaCl crystallites.

De Boer[5] first characterized the absorption of light by molecules adsorbed to alkali halides. Further, he discussed the photolytic behaviour of some of these salts. Since that time numerous investigators[6–9] have studied the effects that defect sites, including colour centres, have on adsorbed or matrix isolated molecules with the alkali halides. The main focus of the present work is the flow of energy following optical excitation. Interest in energy flow has been heightened by experiments showing that light-induced self trapped excitons (STEs) in the NaCl(100) substrate transfer their energy to adsorbed acetylene (C_2H_2) molecules, thus initiating photochemistry.[10,11] Here work on the NaCl(100) surface is continued by exploring the photochemistry of ethene (C_2H_4) physisorbed onto a polycrystalline film of NaCl formed by sublimation.

Background

Ethene: electronic states and photochemistry

The electronic spectra,[12–15] excited states[13–18] and photochemistry[19–33] of ethene have been studied extensively. The planar ethene molecule (D_{2h}) in its ground state, N, has the term symbol ^1A_g, while the first optically accessible (electric dipole allowed) singlet excited state, V, is labeled $^1B_{1u}$. In the V state the molecule is twisted, with a 90° dihedral angle between methylene groups. The V–N transition appears in the gas-phase as a diffuse absorption around 215 nm. The optical cross-section of this π^*–π transition increases rapidly with decreasing wavelength to a maximum at 162 nm. The triplet component of the π^*–π transition, the lower lying T($^3B_{1u}$) state, is shown in comparison to the N and V states in Fig. 1.

† Present address: Department of Nutrition and Food Science, Auburn University, Auburn, AL 36849, USA.
‡ Present address: Department of Chemistry, University of California, Riverside, CA 92521, USA.

The primary photodissociation channels of gas-phase ethene (between 123.6 and 193 nm) occur *via* molecular H_2 elimination

$$C_2H_4^* \rightarrow HC{\equiv}CH + H_2 \quad (1a)$$

$$\rightarrow H_2C{=}C{:} + H_2 \quad (1b)$$

and H-atom elimination

$$C_2H_4^* \rightarrow H_2C{=}CH^{\cdot} + H^{\cdot} \quad (2a)$$

$$\rightarrow HC{\equiv}CH + 2H^{\cdot} \quad (2b)$$

where $C_2H_4^*$ represents photoexcited ethene.[19–28] It has been shown,[28] however, that as the energy of the exciting photon is increased, atomic detachment (2) is slightly enhanced. In any event the ratio of reactions (1) : (2) is roughly 1 : 1 at all wavelengths.[25]

In molecular elimination (1) the branching ratio of acetylene to vinylidene (1*a* : 1*b*) is 2 : 3.[25] With the use of isotopes it has been shown[19,21] that photoexcited ethene, $C_2H_4^*$, can freely rotate about the C—C bond and that either 1,1 or 1,2-H_2 elimination is possible. It has also been conjectured[19] that the acetylene pathway (1*a*) may proceed *via* an ethylidene, H_3C—CH, intermediate.

The mechanism for H-atom elimination is better understood.[25,27] After photoexcitation, $C_2H_4^*$ internally converts to vibrationally excited states in the ground electronic level and

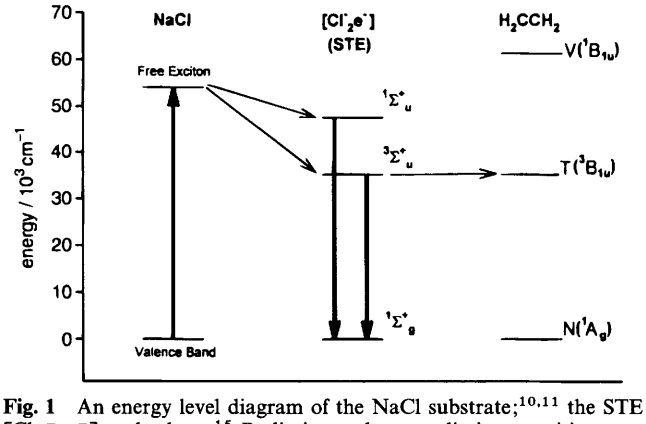

Fig. 1 An energy level diagram of the NaCl substrate;[10,11] the STE [Cl_2^- e^-] and ethene.[15] Radiative and non-radiative transitions are shown with large and small arrows, respectively. The high energy-edge of each STE luminescence band has been used as a lower limit for the energy levels shown.[10,11] Vertical transition energies have been used for the ethene T and V states.[15]

subsequently undergoes elementary bond rupture. Vinyl radical is produced [reaction (2*a*)], some of which has sufficient internal energy to decompose into acetylene and another H atom. Minor products which have been observed in gas-phase photolysis following 184.9 nm excitation[20,21,23] are but-1-ene, *n*-butane and ethane, which originate *via* the atomic hydrogen detachment pathway (2).

In the liquid phase (using 184.9 nm photons) it has been shown that the atomic elimination pathway is quenched: the ratio of the H atom, route (2), to H_2 molecular elimination, reaction (1), is 0.03 to 1.[30] Further, in all condensed phase (solid[29,30] or liquid[30]) photolysis experiments (123.6–184.9 nm), the ratio of product acetylene to product H_2 has been found to be *ca.* 1 : 1; *i.e.* in the condensed phase photolysis, reaction (2), is not important. When solid ethene is photolysed at 184.9 nm,[29,30] besides the main products of acetylene and H_2, minor species formed are but-1-ene, *n*-butane, methyl cyclopropane, cyclobutane and buta-1,3-diene. These trace constituents are a consequence of secondary reactions involving radical products of reactions (1) and (2).

Photochemistry on the NaCl(100) surface

The photochemistry of adsorbed molecules can be modified by static or dynamic effects. Shifts in electronic or vibrational levels, examples of a static effect, reflect perturbations of the molecular structure by the alkali halide substrate. The alteration of relaxation pathways of the excited molecule is a dynamic effect.

Perturbation of the ground electronic state of a physisorbed molecule is usually weak, as evinced by the relatively small vibrational frequency shifts. Pure vibrational transitions of adsorbates on NaCl occur within 1% of their gas-phase energies. On the other hand, the electronic properties responsible for adsorption can be quite different in excited electronic states. Thus the energetics of excited-state adsorption can modify the optical transitions among these states. Large 'solvent shifts', the inhomogeneous loss of vibronic structure, and enhanced optical cross-sections have been observed in the spectra of ketene and acetylene on NaCl.[34,35] An extreme example of static influence involves a spontaneous chemical reaction between the ground states of an adsorbate and a lattice defect. Smart and Jennings[6] first pointed out that the absorbance due to colour centres in polycrystalline films of NaCl and NaF was bleached by the adsorption of NO molecules onto the surface. They found IR spectral evidence of NO^- and NO^+ species, the result of reaction with F and V colour centres at the surface. Zecchina and Scarano[7] saw similar behaviour when CO was adsorbed to a film of KCl where they found CO^- and CO^+. Michl and co-workers[8] have described a number of photochemical experiments of organic molecules co-deposited in films of alkali halides. The photochemistry of these matrix-isolated species are directly affected by colour centres and defects. The novel chemistry occurs by direct optical excitation of the newly mixed electronic resonances.

Colour centres can also influence photochemical reactions dynamically, by acting as source or sink of excitation energy for independent adsorbates. Leggett *et al.*[9] have suggested that defects in bulk LiF can transfer enough energy from an optical pump to dissociate adsorbed OCS. Dunn and Ewing[10,11] have documented the influence of self-trapped excitons in NaCl (STEs) on the photochemistry of adsorbed acetylene. Fig. 1 is an energy level diagram that locates the STEs among other relevant states. Upon excitation at 184.9 nm a bound electron–hole pair, or exciton, is created. An exciton, which is initially associated with a single halide ion (Cl^-), is free to travel throughout the crystal. Coupling between a free exciton and lattice modes results in the formation of a covalently bonded Cl_2^- and a nearby electron, indicated by [Cl_2^- e^-], called a self trapped exciton (STE). Recombination of the electron and Cl_2^- of the STE results in the intrinsic luminescence observed in alkali halides.[36–40] This emission consists of two bands; one from a high energy, short-lived state (*ca.* 10^{-9} s) and the other from a low energy, long-lived state ($>10^{-6}$ s). The corresponding electronic states are essentially a singlet and a triplet.[38] These states resemble those of a diatomic rare gas molecule, and can be labelled $^1\Sigma_u^+$, $^3\Sigma_u^+$ as indicated in Fig. 1.

In alkali halides at low temperature, STEs will always play a role in the dissipation of sufficiently energetic optical excitations.[41,42] These states can migrate and transfer energy over distances as large as the dimensions of the NaCl particles in our films.[43–45] Also, STEs unique to the surface can exist at slightly lower energies than in the bulk.[46] Trapping at the surface is caused by either intrinsic capture sites[47,48] or by extrinsic sites,[49] where these extrinsic sites might be adsorbed molecules. Thus, electronic excitation of a polycrystalline NaCl film is a store of potential chemical energy, energy which can likely be transferred to the molecules adsorbed on its surface.

In a series of experiments[10,11] it was established that triplet STEs ($^3\Sigma_u^+$) are formed at the NaCl surface and that their energy was transferred to adsorbed acetylene molecules creating the excited state $C_2H_2(^3\Sigma_u^+)$. Luminescence from the triplet STE state was effectively quenched when acetylene was adsorbed onto the NaCl substrate. A surface diffusion-limited hydrogen-exchange reaction then proceeded *via* this excited acetylene triplet state.[35] A diffusion limited reaction implies a long excited state acetylene lifetime ($\geqslant 1$ μs) as expected for a triplet state. Hence, for acetylene its photochemical dynamics are strongly influenced by the NaCl substrate while, as already mentioned, its static behaviour (the actual shape of the excited state potential surface accessible by 184.9 nm photons) seems little affected.

These photochemical studies are now expanded to ethene on the NaCl(100) surface. Referring to Fig. 1 it can be seen that there is also a close match in energy between the NaCl STE($^3\Sigma_u^+$) and the first ethene triplet state T($^3B_{1u}$). Triplet–triplet energy transfer has been studied rather extensively[50] in frozen matrices[51] and in gas-phase ethene[52] and dideuterioethene.[53,54] A goal of this work will be to explore whether the NaCl surface also plays an active role in ethene photochemistry.

Experimental

NaCl films

Films consisting of aggregated cubic crystallites (*ca.* 100 nm on edge) with (100) faces exposed[44,45] were prepared in an apparatus that we have previously described.[34,44] The cell was fitted with barium fluoride windows, that are transparent through the mid-IR and into the UV. Gas pressure in the cell was monitored by an MKS Baratron capacitance manometer, which was accurate to within 5% ($\pm$0.001 mbar at low pressures). The temperature of the cell could be varied from 20 to 300 K. This was measured with a thermocouple, that in turn was calibrated against the vapour pressure of neat liquid ethene and N_2.

Adsorption isotherms on the film were obtained by an aliquot method. Ethene gas (Air Products c.p. grade 99.8% pure) and CO (Matheson Gas) were used without further purification. A sample of gas was expanded into a vacuum manifold, whose volume was known, and the pressure recorded. Thus, a known amount of gas molecules were in the vacuum manifold. The sample cell was then exposed to the manifold and allowed to equilibrate. The number of molecules adsorbed on the surface could be calculated from the number of gas molecules remaining. Consecutive doses allowed for a plot of the number of molecules adsorbed *vs.* the equilibrium vapour pressure.

Spectroscopy

IR spectra were recorded with a Fourier-transform IR spectrophotometer (Mattson Nova Cygni 120), at a nominal resolution of 2 cm^{-1}. A room-temperature TGS detector covered the range from 4000 to 700 cm^{-1}. Each single-beam spectrum contained 500 coherently averaged scans. Absorbance, $A = \log(I_0/I)$, was computed as a function of wavenumber, $\tilde{\nu}/cm^{-1}$, with an appropriate background spectrum. The integrated area under spectroscopic bands is defined as $\tilde{A} = \int_{band} \log(I_0/I)d\tilde{\nu}$.

A UV–VIS spectrophotometer (Cary 14R) was used to record the electronic spectra between 400 nm and the small wavelength cut-off of the instrument, at 190 nm. To obtain absorbance measurements at 184.9 nm, a 4.6 W low-pressure mercury discharge lamp [Oriel Hg(A) model 6035] was used as the source. Radiation from these lamps is primarily through two mercury resonance lines at 184.9 and 253.7 nm.[34] To select only 184.9 nm photons a narrow band interference filter (peak 185 nm, FWHM 27 nm, Acton Research Corporation) was placed in front of the lamp. The light was further filtered by a monochromator (Bausch & Lomb model 33-86-02, grating of 1350 grooves mm^{-1}); 184.9 nm photons were selectively passed using the grating in third order at 555 nm. After passing through the sample cell, light was collected by a photomultiplier tube (PMT, Burleigh IP28). The lamp, monochromator, sample cell and PMT were purged with dry N_2 gas.

Adsorbed ethene photolysis

The optical set-up for photochemistry of an adlayer has been described in detail.[34] Photolysis of an ethene adlayer was executed with the Hg(A) discharge lamp. The lamp, used without filtering, was placed just above the IR optical path. The sample cell was alternately raised to the lamp for UV irradiation and lowered back into the IR beam for subsequent vibrational spectral analysis. Nine photolysis periods of *ca.* 15 min duration were applied.

After completion of the photolysis, the film was slowly warmed to 80 K with spectra taken at each 10 K increment. During this warming period the cell was opened to the vacuum manifold and the vapour pressure over the film was measured.

Results

Isotherms/characterization of NaCl films

A large number of NaCl films have been prepared in our laboratory and their properties can be closely controlled.[44,45,55] The results from four different films are discussed: film 1 (weighing 57.4 mg) was used for characterization of the ethene isotherms and their IR spectroscopy, films 2 (36 mg) and 3 (49 mg) for UV-absorption spectroscopy and film 4 (20.5 mg) for the photochemical experiment.

Fig. 2 displays the isotherms of ethene on film 1 at 110 K and 119 K. Shown also is an isotherm of CO at 83 K on the same film. The number of molecules adsorbed is plotted *vs.* the equilibrium pressure. The smooth curves shown for the ethene isotherms are fits of the experimental data to the BET (Brunauer–Emmett–Teller[56]) isotherm model, while the CO data was fitted to the Langmuir[44,45] model. These models are discussed in detail below. For the CO isotherm, since no more CO molecules adsorb to the film beyond a pressure of 2 mbar, we conclude that the available adsorption sites are saturated. The relative coverage is designated by $\Theta = N/N_m$, where N is the number of molecules adsorbed and N_m is the number of molecules in a saturated monolayer. Thus at 2 mbar and beyond, the CO isotherm has reached $\Theta = 1$. In contrast, however, the adsorption of ethene molecules continues with increases in equilibrium pressure (*i.e.* coverage continues past

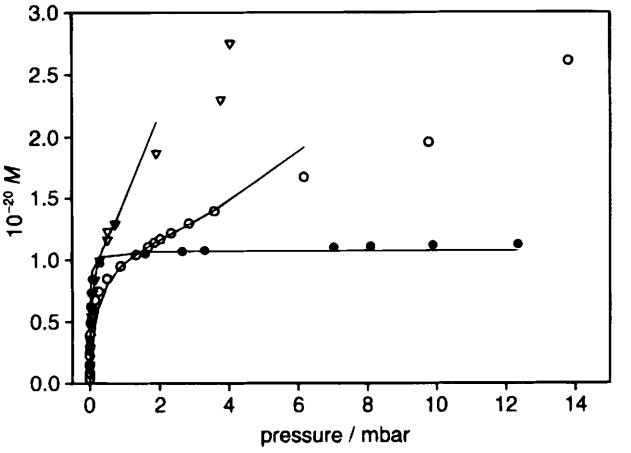

Fig. 2 Isotherms of CO (●) adsorbed at 83 K to a film (film 1) of NaCl crystallites and ethene adsorbed at 119 (○) and 110 K (▽)

$\Theta = 1$). In particular at 110 K, ethene adsorbs until the saturated vapour pressure is reached at *ca.* 4 mbar.[57] Here the isotherm makes a vertical rise corresponding to the onset of condensation. For both ethene and CO, adsorption is a reversible process; reduction of the equilibrium pressure lowers the number of molecules adsorbed to the film. This reversibility is reflected by changes in the integrated absorbance, $\tilde{A}$, of spectroscopic features in the IR spectra.

IR spectroscopy

Fig. 3 is a mid-IR survey spectrum of ethene at 110 K on film 1. The coverage in this spectrum is $\Theta = 0.55$ ($N = 6.1 \times 10^{19}$ molecules, with $2.0 \pm 0.4 \times 10^{18}$ of these molecules actually adsorbed on the portion of the film that has been deposited on the windows of the sample cell). There are nine sharp features whose frequencies are listed in Table 1, as well as two weak diffuse bands at 1909 and 2048 cm^{-1}. The absorbance of all eleven features is reversible with changes in pressure and the band positions shift little with coverage. The sublimed NaCl film acts as an etalon giving the rolling background in Fig. 3.

At low ($\Theta < 0.2$) and multilayer coverages ($\Theta > 1.0$), however, the profiles of some bands reflect differences in the morphology of the NaCl film and the ethene adlayer. Fig. 4 shows spectra of the ethene absorbance centred between 1000 and 900 cm^{-1} to illustrate these changes. At low coverage, $\Theta = 0.01$, there is only one peak present, at 987 cm^{-1}, with a broad trailing absorbance extending to 960 cm^{-1}. At a slightly higher coverage, $\Theta = 0.03$, there are three distinct features;

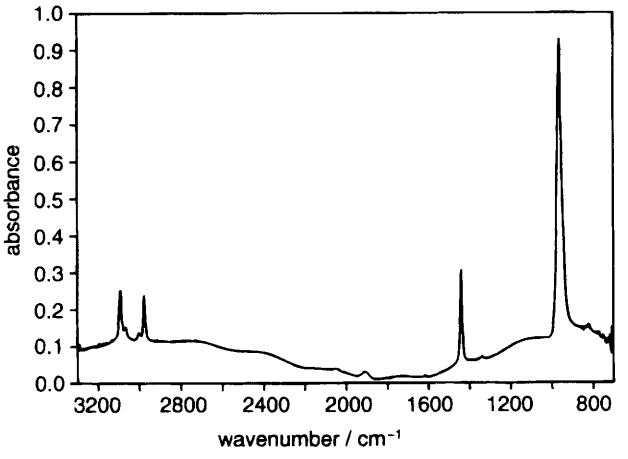

Fig. 3 A mid-IR survey spectrum of ethene adsorbed to a film (film 1) of NaCl crystallites at 119 K and a coverage of $\Theta = 0.55$ (6.1×10^{19} molecules with $2.0 \pm 0.4 \times 10^{18}$ on the windows)

Table 1 Vibrational spectroscopy of ethene with peak positions in wavenumbers, $\tilde{\nu}/cm^{-1}$

mode	gas[a]	solid[b,c]	matrix[d]	NaCl(100) single crystal[e]	film[g]
$\nu_1(A_g)$	3026	3000.5 2997.0	3015	—	3001
$\nu_2(A_g)$	1623	1615.5 1602	1623	—	1618
$\nu_3(A_g)$	1342	1348.0 1331.2	1334	—	1340
$\nu_4(A_u)$	1023	1041.9 1036.0	1028	—	—
$\nu_5(B_{1u})$	2989	2972.9 2965.7	2984 2975	2981	2976
$\nu_6(B_{1u})$	1444	1440.2 1436.0 1434.0	1438.5	1441	1439
$\nu_7(B_{2g})$	943	949.6 941.4	—	—	—
$\nu_8(B_{2u})$	3106	3092.2 3088.0	3098 3090	3097.4	3092
$\nu_9(B_{2u})$	826	825.8 822.5 819.5	824 820	—	822
$\nu_{10}(B_{3g})$	3103	3067.3 3061.0	—	—	3068
$\nu_{11}(B_{3g})$	1236	1226.7[f] 1222.4	1227	—	—
$\nu_{12}(B_{3u})$	949	953.0 948.9 941.1 937.0	951	968.2	965

[a] Ref. 64. [b] Ref. 65. [c] Ref. 66. [d] Ref. 67. [e] Ref. 61. [f] Ref. 82. [g] This work.

the peak at 987 cm^{-1}, and weaker bands at 977 and 968 cm^{-1}. By a coverage of $\Theta = 0.15$, the bands at 987 and 977 cm^{-1} appear only as shoulders to the main absorbance at 968 cm^{-1}. Moreover a feature at 951 cm^{-1} is beginning to develop. The feature at 968 cm^{-1} then dominates throughout the range $0.2 < \Theta < 0.9$, shifting slightly to 965 cm^{-1} with the 951 cm^{-1} feature appearing as strong shoulder on the $\Theta = 0.89$ spectrum. Finally, the feature at 951 cm^{-1} dominates when $\Theta = 1.2$.

UV absorption spectroscopy

The UV absorbance spectrum of 100 mbar of gas-phase ethene in the sample cell (pathlength 3.85 cm) was collected with the UV spectrophotometer, and the absorbance at 184.9 nm was recorded at with the Hg(A) lamp and PMT apparatus. The gas-phase absorbance spectrum showed one diffuse contour originating at *ca.* 200 nm that rose sharply to the small wavelength cut-off at 190 nm. The absorbance measured for 100 mbar of gas at 184.9 with the Hg(A) lamp and PMT was 0.66. After deposition of film 2, an absorbance was observed beginning near 230 nm and rising steadily to 190 nm. This steep absorption profile is due to the film scattering and absorbing light. Spectra of ethene adsorbed onto film 2 between 20 and 119 K at a coverage of $\Theta = 0.22$ ($N = 2.2 \times 10^{19}$ molecules, with $7.0 \pm 1.7 \times 10^{17}$ on the windows) showed the beginning of ethene absorption near 200 nm with no other features at longer wavelengths. In order to measure the absorbance of the ethene adlayer and the NaCl substrate at 184.9 nm, the Hg(A) lamp and PMT were used again. After deposition of film 3 the measured absorbance at 184.9 nm of this bare film was 0.3 ± 0.1, and for the ethene adlayer at $\Theta = 0.20$ (1.2×10^{19} molecules with $3.8 \pm 1.0 \times 10^{17}$ on the windows), $A = 0.089 \pm 0.031$.

Adsorbed ethene photolysis

Film 4 was used for the photolysis experiment. After characterization with CO, it was dosed with ethene at 105 K to a coverage of $\Theta = 0.23$ ($N = 9.7 \times 10^{18}$ molecules, with $3.1 \pm 0.8 \times 10^{17}$ on the sample cell windows). This film was then cooled to 20 K and the lower set of infrared spectra shown in Fig. 5 were taken. A series of nine photolysis periods followed by IR interrogation ensued. After the last photolysis period (195 min total of UV exposure) the upper set of infrared spectra shown in Fig. 5 were taken.

As can be seen in Fig. 5, depletion of the ethene peaks at 965, 1340, 1439, 3068 and 3092 cm^{-1} appears to be uniform. Product features, marked with an asterisk for clarity, are listed in Table 2. It is difficult to distinguish what happens to the ethene peaks at 3001 and 2976 cm^{-1}, because in the upper spectrum they appear to have roughly the same intensity as in the lower spectrum. However, in the upper spectrum the feature at 3001 cm^{-1} is shifted to 3005 cm^{-1} and the 2976 cm^{-1} feature shows a bandwidth and profile change. Since all of the other ethene bands deplete rather uniformly, we assume

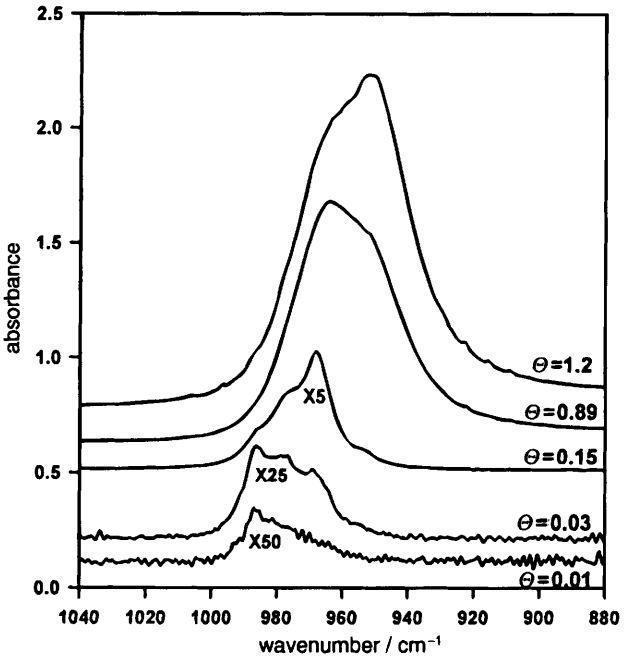

Fig. 4 IR spectra of the features centred at 968 cm^{-1} of ethene adsorbed to a film of NaCl crystallites at 110 K and various coverages. The low-coverage spectra ($\Theta = 0.01$ and 0.03) are from film 4, while the rest are from film 1.

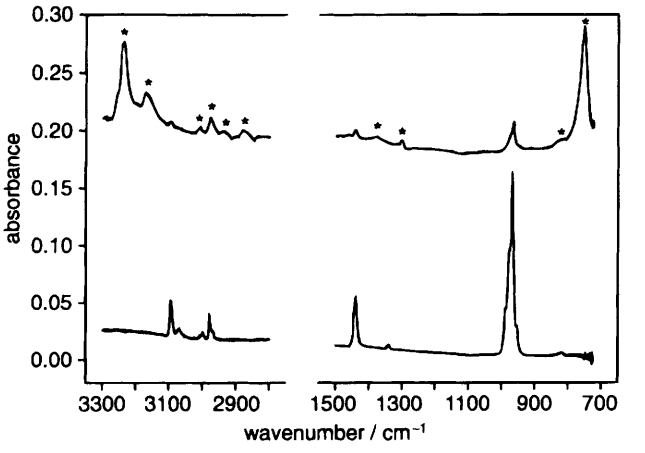

Fig. 5 IR spectra of ethene adsorbed to a film (film 4) of NaCl crystallites at 20 K, coverage of $\Theta = 0.23$ (9.7×10^{18} molecules with $3.1 \pm 0.8 \times 10^{17}$ on the sample cell windows), and its photolysis products. The lower set of spectra is ethene only, before 184.9 nm irradiation, while the upper traces are after 195 min of irradiation.

Table 2 IR bands of the products observed in the photolysis of ethene on NaCl

observed peak position (cm^{-1})	possible species				
	C_2H_2 (acetylene)[a]	$-CH_3$ group[b]	$-CH_2$ group[b]	$H_2C{=}C{:}\ (^3B_2)$[c]	$H_3C{-}CH\ (^3A'')$[d]
3240	ν_3 (smooth face)[a]				
3170	ν_3 (defect sites)[a]				
3005				$\nu_5(b_2)$ asym stretch (3000 cm^{-1})	$-CH_3$, C—H stretch (3072 cm^{-1})
2976		asym stretch (2962 cm^{-1})			$-CH_3$, C—H stretch (2975 cm^{-1})
2950			asym stretch (2926 cm^{-1})	$\nu_1(a_1)$ sym stretch (2930 cm^{-1})	$-CH_3$, C—H stretch (2942 cm^{-1})
2875		sym stretch (2872 cm^{-1})			$-CH$, C—H stretch (2875 cm^{-1})
1380	$\nu_4 + \nu_5$	sym bending (1375 cm^{-1})		$\nu_3(a_1)$ CH_2 scissors (1375 cm^{-1})	$-CH_3$ wag (1412, 1406, 1348 cm^{-1})
1302					$-CH_3$ wag (1300 cm^{-1})
825	$\nu_5 + \nu_t$			$\nu_4(b_1)$ out-of-plane (775 cm^{-1})	
752	ν_5				

[a] Ref. 35. [b] Ref. 83. [c] Ref. 77. [d] Ref. 71 and 84. The frequencies for $^3A''$ have been adjusted for anharmonicity by multiplying the authors' harmonic values by 0.93. The authors suggest that the true fundamental vibrational frequencies are *ca.* 7–10% less than their given harmonic values.

that the signals at 3005 and 2976 cm^{-1} in the upper spectrum are due to photolysis products. The very weak ethene feature at 822 cm^{-1} in the bottom spectrum is buried by a broad shoulder in the upper spectrum at 825 cm^{-1}, but again we assume the ethene peak at 822 cm^{-1} depleted uniformly and that the 825 cm^{-1} signal is due to products.

After the upper spectra in Fig. 5 were taken, and the photolysis was essentially complete, the film was slowly warmed to 80 K. Spectra collected at each 10 K increment changed little during this warming but, at 40 K, gas started to appear in the manifold. Above 40 K H_2 desorbs from the NaCl surface.[55] At 80 K the total amount of gas in the cell/manifold corresponded to 3.7×10^{17} molecules. This is within the error limit of the original $3.1 \pm 0.8 \times 10^{17}$ ethene molecules adsorbed on the windows of film 4.

Discussion

Isotherms/characterization of NaCl films

The isotherms in Fig. 2 are analysed with two specific models for the adsorption of molecules to surfaces; the Langmuir[44,45] and the Brunauer–Emmett–Teller (BET).[56] The Langmuir isotherm describes adsorption to discrete, independent sites. It is expressed by the equation

$$\Theta = \frac{kp}{1 + kp} \tag{3}$$

where the extent of the coverage is represented by the parameter, $\Theta = N/N_m$, p is the equilibrium vapour pressure of the adsorbing gas above the surface, and k is an effective equilibrium constant for the adsorption process. The Langmuir model has been shown accurate for CO on NaCl.[44,45] A variety of experimental and theoretical studies show that CO adsorbs over the Na^+ ions on the NaCl surface with negligible lateral interactions within the adlayer. Thus, the number of Na^+ (as well as Cl^-) surface sites is N_m. For film 1, N_m was determined to be $1.1 \pm 0.1 \times 10^{20}$ from a fit of the CO data to the Langmuir curve shown in Fig. 2.

For other molecules[58–60] including C_2H_4,[61] adsorbate–adsorbate interactions are significant and different models are required to describe their isotherms. A model which takes multilayer growth into account is the BET theory.[56] Its isotherm is represented by

$$\Theta = \frac{cz}{(1 - z)[1 - (1 - c)z]} \tag{4}$$

where $z = p/p_0$, with p_0 the vapour pressure of the bulk adsorbate. The parameter c is a measure of the relative probability of adsorption in the first and subsequent layers. It is defined by

$$c = \exp\left[-\frac{E_m - E_l}{RT}\right] \tag{5}$$

where E_m is the site energy for molecules in the first layer (monolayer) and E_l is the site energy of molecules in subsequent layers (multilayers).

The isotherms of ethene on film 1 at 110 and 119 K were fitted to the BET equation, yielding the curves shown in Fig. 2. The values obtained for N_m were $1.1 \pm 0.1 \times 10^{20}$ at both 110 and 119 K, identical to that determined from the CO isotherm. Ethene, therefore, bonds in a one-to-one correspondence to Na^+ (or Na^+ Cl^- pairs) just like CO. Further, the ethene adlayer is clearly influenced by adsorbate–adsorbate interactions on the NaCl surface. In systems for which $c > 50$ the initial layer is more or less complete before multilayer formation begins. The values for c obtained in this study were 72 ± 11 and 68 ± 19 (at 119 and 110 K, respectively). This indicates that ethene should form a complete monolayer before multilayers appear.

The heat of adsorption, $\Delta_{ads}H$, can be calculated by applying the Clausius–Clayperon equation

$$\left[\frac{\partial(\ln K)}{\partial T}\right]_\Theta = \frac{-\Delta H_{ads}}{RT} \tag{6}$$

to the two ethene isotherms at various coverages. The heat of adsorption is $-10 \pm 3 < \Delta_{ads}H < -17 \pm 3$ kJ mol^{-1} for $0.5 < \Theta < 1.0$, which roughly matches a value we have previously measured for ethene adsorbed onto a single crystal of NaCl.[61] These values are also in the range generally observed for small molecules on NaCl films.[62,63]

Vibrational assignments: ethene

Table 1 summarizes the positions of ethene features in the IR survey scan (Fig. 3), and assigned to fundamental transitions below. Also listed in Table 1 are assignments from the gas,[64] solid,[65,66] rare-gas matrix[67] and on NaCl(100) single crystal.[61] The molecular z axis is along the C=C double bond, while the x axis is perpendicular to the molecular plane.[61] The symmetry labels in Table 1 are consistent with this coordinate system as are the notations used for the electronic states.

We focus first on the six ethene ungerade modes ν_4, ν_5, ν_6, ν_8, ν_9 and ν_{12}. The symmetry of the isolated ethene molecule is D_{2h} and in the gas-phase all ungerade modes are predicted to be IR active. Referring to Table 1, assignment of five of these six fundamental modes to features in Fig. 3 is unambiguous. Their frequencies are nearly identical to the corresponding solid and matrix forms. Further, upon condensation into the liquid, solid or matrix, or on adsorption to the NaCl surface, the vibrational frequency is shifted by only $\approx 1\%$ from the gas. It is clear, therefore, that the weak feature at 822 cm^{-1} is ν_9, the strong band at 965 cm^{-1} is ν_{12} and the three relatively strong bands at 1439, 2976 and 3092 cm^{-1}, are ν_6, ν_5 and ν_8, respectively. Note that not only are the location of these bands similar to gas, solid and matrix values, their relative intensities are nearly the same as well: *i.e.* the ν_9 oscillator strength (its integrated infrared cross-section) is $\approx 10^{-2}$ of ν_{12} while ν_6, ν_5 and ν_8 are $\approx 10^{-1}$ of ν_{12}. In the solid,[65] the oscillator strength of ν_4 is $\approx 10^{-3}$ of ν_{12}, and thus it is no surprise that it is not seen on the NaCl film.

Two combinations modes were also observed on the film, $\nu_{11} + \nu_9$ at 2048 cm^{-1} and $\nu_{12} + \nu_7$ at 1909 cm^{-1} (both of which have ungerade symmetry) and their assignment based on comparison to gas and solid-phase values is unambiguous as well.

We turn now to the fundamental gerade modes, ν_1, ν_2, ν_3, ν_7, ν_{10} and ν_{11}, that in D_{2h} symmetry are only Raman active. Strong electric fields near the ionic surface, by lowering the point-group symmetry, can induce IR activity in these modes as it does for H_2 on NaCl.[55] For physisorbed ethene, assignment of the weak absorptions at 3001, 1340 and at 1618 cm^{-1}, respectively, to ν_1, ν_3 and ν_2 seems reasonable. ν_{11} was not observed, but even in Raman spectra of the gas and solid phase[66] it has inherently low intensity. ν_7, if present, is buried in the broad absorption of ν_{12}. It is unclear whether the signal at 3068 cm^{-1} is ν_{10} or the $\nu_2 + \nu_6$ combination mode. The latter is weak but clearly evident in the solid.[66] Since ν_1, ν_2 and ν_3 were observed, however, and they all have roughly the same absorbance in the gas and solid, it seems reasonable to believe that it is ν_{10}.

We focus specifically now on the out-of-plane bending mode ν_{12} which is shown at various coverages in Fig. 4. Characterization of our films in the past has led to the conclusion that, in general, as much as 20% of the film surface may be defect sites.[55] At $\Theta < 0.2$ an individual mode may show many distinct features associated with these defects. The ν_{12} adsorption can be used as a probe of surface site heterogeneity. The features at 987 and 977 cm^{-1}, which are most prominent at $\Theta = 0.01$ and 0.03, are associated with ethene molecules adsorbed to energetic defect sites (perhaps the edges of steps or terrace vacancies). By $\Theta = 0.15$ these features become obscured as adsorption to the main smooth face sites, the feature at 965 cm^{-1}, takes over. This assignment is justified by the similar frequency of C_2H_4 on single-crystal NaCl(100).[61] The shoulder at 951 cm^{-1} which appears at $\Theta = 0.89$ and continues to grow when $\Theta > 1$ is naturally associated with the formation of bulk ethene. Since in the IR spectra of solid ethene[65] the main feature of the ν_{12} band is found at 953 cm^{-1}.

According to this analysis of the ν_{12} mode, at the coverage of the photolysis experiment ($\Theta = 0.23$) the C_2H_4 molecules are principally adsorbed to smooth faces. Their adsorbed structure should closely resemble that of ethene adsorbed onto the single crystal NaCl(100) faces.[61]

Vibrational assignments: photolysis products

Table 2 summarizes the positions of all product features seen in the top spectrum of Fig. 5. Of these only three can be associated with acetylene. The strong bands at 3240 and 3170 cm^{-1} have previously been identified as due to its ν_3 stretching mode.[35] The strongest band, at 3240 cm^{-1}, arises from smooth faces of the NaCl crystallites, while the weaker band at 3170 cm^{-1} arises from defective sites. The other strong absorption, at 752 cm^{-1}, is assigned to ν_5 based on comparison to gas[64] and solid[68–70] acetylene spectra. The features at 1380 and 825 cm^{-1} are consistent with the combination bands $\nu_4 + \nu_5$ and $\nu_5 + \nu_6$, respectively; other candidates for their assignment are suggested in Table 2.

Identification of the remaining features is difficult. Instead of assigning these features to specific modes of a particular molecule, comparison to functional group frequencies will be used to choose appropriate molecular species and eliminate others. Hence in Table 2, frequencies for various groups that may be found in the photolysis products are listed. Further, it will be seen below that the ethylidene and vinylidene intermediates play key roles. A vast amount of theoretical[32,71–74] and some experimental[75–77] work has been done on these species. These studies show that ethylidene and vinylidene are both stable intermediates, *i.e.* they can reside in potential energy minima and are not just saddle points in their respective potential energy surfaces. Calculated and observed vibrational frequencies are placed next to appropriate peaks observed in our experiment in Table 2. We see that many of the weak unassigned features at 3005, 2976, 2950, 2875 and 1302 cm^{-1} may be associated with these intermediates. Ethene dimer (C_4H_8) and products from the reaction of $C_2H_4^*$ with C_2H_4 are also candidates. The most likely choice would be but-1-ene. The strong in- and out-of-plane CH_2 wagging mode for but-1-ene is found in the gas phase at 912 cm^{-1}. This mode would be expected near 900 cm^{-1} on the NaCl surface; it is not present in the spectra of Fig. 5. Ethane (C_2H_6) and *n*-butane (C_4H_{10}) would have the observed CH_3 and CH_2 stretching and bending modes listed in Table 2. However, their vinyl radical precursor is excluded on energetic grounds (below). The key spectroscopic feature of the vinyl radical itself ($H_2C{=}CH^{\cdot}$), when trapped in an argon matrix,[78] is the CH out-of-plane bending mode at 900 cm^{-1} (analogous to the ν_{12} mode at 949 cm^{-1} in ethene; see Table 1). This vinyl radical mode, which is expected to have the greatest oscillator strength, is absent in the top spectra of Fig. 5. We suggest that these unassigned bands are due to ethylidene ($H_3C{-}CH$) and vinylidene ($H_2C{=}CH{:}$) species trapped by adsorption, and perhaps chemically stabilized.

Ethene photometry

For the analysis of the ethene photolysis it will be necessary to determine IR integrated optical cross-sections ($\bar{\sigma}$, cm molecule^{-1}) and a UV optical cross-section (σ, cm^2 molecule^{-1}). The integrated cross-sections will be used to quantify the depletion of ethene and the subsequent formation of product acetylene, while the UV cross-section will allow us to calculate a quantum yield, Φ (molecular dissociation rate/photon absorption rate).

As Berg and Ewing show,[34] the Beer–Lambert law for adsorbed molecules can be expressed as

$$\sigma = 2.303A/N_{2D} \tag{7}$$

where the parameter N_{2D} (molecules cm^{-2})is the density of molecules projected onto a plane normal to the propagation of light and, as before, A is the absorbance. Thanks to our dosing procedure, the number of molecules adsorbed is known. Further, $3.2 \pm 0.8\%$ of the adsorbed sample is on the windows which have an effective diameter of 1.1 cm giving a window area, $A_w = 0.95$ cm^2. Hence N_{2D} can be determined, and σ calculated *via* eqn. (7). To obtain the integrated cross-section, $\bar{\sigma}$, eqn. (7) is integrated over the band profile. The integrated cross-section values for ethene are $\bar{\sigma}(\nu_{12}) = 2.6 \times 10^{-17}$, $\bar{\sigma}(\nu_3) = 6.3 \times 10^{-20}$, $\bar{\sigma}(\nu_6) = 3.7 \times 10^{-18}$, $\bar{\sigma}(\nu_5) = 1.2 \times 10^{-18}$ and $\bar{\sigma}(\nu_8) = 2.7 \times 10^{-18}$ cm molecule^{-1}. An inte-

grated cross-section for adsorbed acetylene comes from previous work in our laboratory, where $\bar{\sigma}(\nu_3) = 2.4 \times 10^{-17}$ cm molecule^{-1}.

The diffuse absorbance we observe in gas-phase ethene near 200 nm is the onset of the V ← N transition. The adsorbed ethene adlayer also has a steeply rising absorbance beginning at 200 nm, which we assign it to the V ← N transition as well. (In crystalline[79] and matrix-isolated[80] ethene, the frequency and cross-section of the V ← N transition correspond closely to the gas.)

To calculate the UV optical cross-section for adsorbed ethene at 184.9 nm we take our measured value of $A = 0.089 \pm 0.031$ together with $N_{2D} = 4.0 \times 10^{17}$ molecules (for film 3) and obtain $\sigma_{\text{adsorbed ethene}} = 5.1 \pm 2.0 \times 10^{-19}$ cm^2 molecule^{-1}. The gas-phase optical cross-section was determined by substituting Nl for N_{2D} in eqn. (7), where N is the density of gas molecules in a pathlength, l, to obtain $\sigma_{\text{gas phase}} = 2.0 \pm 0.5 \times 10^{-19}$ cm^2 molecule^{-1}. Agreement with previously published cross-sections is good.[12,13] Hence, the UV optical cross-section of ethene adsorbed to a film of NaCl crystallites is *ca.* 2.5 times larger than in the gas phase. Clearly, the NaCl substrate is influencing the electronically excited ethene.

The absorbance due to the NaCl crystallites, which was measured to be 0.3 ± 0.1 at 184.9 nm, must now be addressed. Some of the light is lost due to scattering since the dimensions of the crystallites (*ca.* 100 nm) is comparable to the wavelength of the photolysing light. The small decrease in wavelength from 230 to 184.9 nm cannot account for the striking increase that was observed. The measured absorbance of 0.3 ± 0.1 must primarily be due to absorption and not light scattering. Since high-purity crystalline NaCl is transparent at 184.9 nm[81] it is likely that the many defects in polycrystalline films include colour centres. Thus, they are a sink for a significant amount of electronic energy.

Photolysis of adsorbed ethene: stoichiometry

The integrated IR cross-sections ($\bar{\sigma}$, cm molecule^{-1}) will now be used to quantify the photochemical reaction data. If eqn. (7) is integrated over wavenumbers and the window area, a_w, is used, the following expression for the number of molecules adsorbed on the windows, M, results:

$$M = N_{2D} a_w = 2.303 \tilde{A}/\bar{\sigma} \quad (8)$$

The empirical integrated cross-sections were given earlier. Now eqn. (8) gives the number of ethene molecules as a function of time, as shown in Fig. 6. Shown also is the acetylene product formation as a function of time. After the six photolysis periods (111 min of ultraviolet exposure) the mercury lamp was moved from one side of the film cell (entrance window) to the other side of the film cell (exit window). Three more photolysis periods followed, and it is clear that ethene photodepletion and acetylene production continues.

Photolysis of adsorbed ethene: quantum yield

We now calculate the quantum yield of photodissociation, defined as: Φ = molecular dissociation rate (r)/photon absorption rate (P). Since the ethene is effectively transparent to 253.7 nm light, we will assume that all photolysis is a result of the 184.9 nm contribution from the mercury lamp.

The first step will be to obtain r, the initial molecular dissociation rate. With the amount of ethene consumed in the first 15 min (900 s) of Fig. 6, we find $r = 6.7 \times 10^{13}$ molecules s^{-1}. To get the photon absorption rate, P, we first use

$$I = I_0 \exp - (N_{2D} \sigma). \quad (9)$$

The light intensity incident on the adsorbed sample has been determined for our photolysis set-up:[34] $I_0 = 1.5 \times 10^{14}$ photons s^{-1}. Insertion of $N_{2D} = 2.9 \times 10^{17}$ molecules cm^{-2} and $\sigma_{\text{adsorbed ethene}} = 5.1 \pm 2.0 \times 10^{-19}$ cm^2 molecule^{-1} into eqn. (9) yields $I = 1.3 \pm 0.1 \times 10^{14}$ photons s^{-1}, and $P = I_0 - I = 2.0 \pm 1.0 \times 10^{13}$ photons s^{-1}. The quantum yield at 184.9 nm is $\Phi = r/P = 4 \pm 2$ molecules photon^{-1}. Thus for every photon adsorbed by an ethene molecule it would appear that 2–6 are being photolysed.

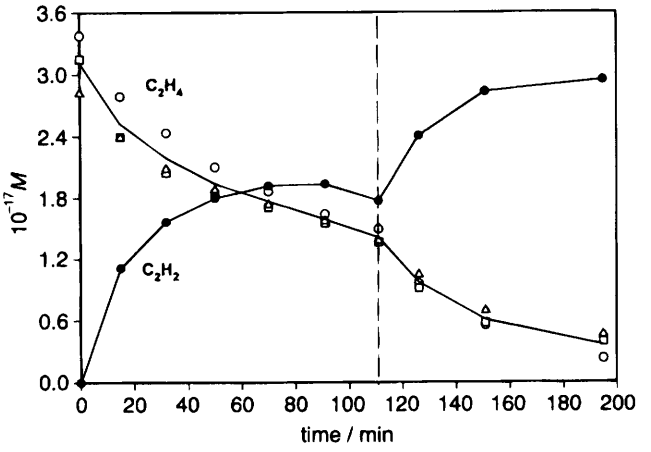

Fig. 6 Photometric survey of ethene photodepletion and product acetylene accumulation on a film (film 4) of NaCl crystallites at 20 K. Ethene bands shown are ν_8 (○), ν_6 (□), ν_{12} (△) while the one acetylene band shown is ν_3 (●). The dashed line at 110 min shows where the Hg(A) photolysis lamp was moved from the window on one side of the film cell apparatus to the window on the opposite side. The lines through the data points are drawn only as an aid to the eye.

Photolysis of adsorbed ethene: mechanism

The goal now is to outline a reasonable mechanism for the photochemistry of ethene on the NaCl substrate. The significant experimental results that need to be addressed are the apparent quantum yield of $\Phi = 4 \pm 2$ and the almost exclusive production of C_2H_2 and H_2 in a 1 : 1 ratio.

Since in all condensed-phase work[29,30] the hydrogen atom elimination channel (reaction 2) is quenched, the analysis will begin by assuming that ethene on NaCl is photodissociating through H_2 elimination only. The observed C_2H_2 : H_2 ratio of 1 : 1 supports the molecular H_2 elimination mechanism, eqn. (1).

One way to account for $\Phi = 4 \pm 2$ is to assume that the NaCl substrate is passing energy to the adsorbed ethene molecules. As suggested in the introduction, triplet–triplet energy transfer is a strong possibility. Since the NaCl substrate is in fact adsorbing photons, STEs are likely transferring energy to adsorbed ethene, creating the $T(^3B_{1u})$ state.

In Fig. 7 an energy level diagram is displayed for the important photochemical species and intermediates in the reaction $C_2H_4 \rightarrow C_2H_2 + H_2$. On the lhs ethene is shown in its singlet excited state as a result of the direct absorption of 184.9 nm (54 045 cm^{-1}) light, while excitation to the ethene triplet state $T(^3B_{1u})$ from the NaCl substrate is shown below. Products accessible from the ethene triplet state include both the ethylidene $^3A''$ triplet state and the vinylidene $^3B_2$ and $^3A_2$ triplet states. The vinyl radical, however, can only be produced from the ethene singlet state. Direct hydrogen atom elimination requires more energy than is available from the ethene triplet. This diagram also reveals that it is impossible for absorption of 184.9 nm light by ethene to give a quantum yield of dissociation >2. One photon at 184.9 nm has only enough energy to destroy one ethene molecule through the vinyl radical path, and most to only deplete two ethene molecules through ethylidene or vinylidene.

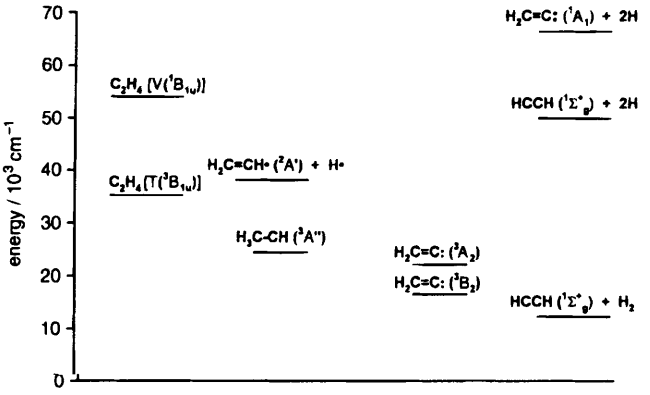

Fig. 7 Energy level diagram of ethene in either the V or T excited state, and the possible pathways for its decomposition. The V state is shown at 54045 cm^{-1} (*i.e.* direct absorption of a 184.9 nm photon) instead of at its vertical transition energy as in Fig. 1. Energies of the vinyl radical (H_2C=CH· = H) and the H-atom elimination states (H_2C=C: + 2H and HC=CH + 2H) come from ref. 85 and 86. The triplet ethylidene state, H_3C—CH ($^3A''$), and the triplet vinylidene states, H_2C=C: ($^3B_2$ and $^3A_2$) are found in ref. 84 and 73, 77 respectively.

An estimate for the amount of energy transfer from the NaCl substrate to the ethene molecules can be made. Film 3 (used for UV absorbance measurements) and film 4 (used for photolysis) were similar, *i.e.* roughly the same amount of salt was deposited and $N_m \approx 6 \times 10^{19}$ sites for both. For film 3 an absorbance of 0.3 ± 0.1 at 184.9 nm was measured for the bare NaCl substrate. If it is assumed that film 4 (used for the photolysis experiment) absorbs roughly same amount of light then, using arguments for the quantum efficiency outlined above, $I = 7.7 \pm 1.8 \times 10^{13}$ photons s^{-1} and $P = 7.3 \pm 1.8 \times 10^{13}$ photons s^{-1}. Since only $P = 2.0 \pm 1.0 \times 10^{13}$ photons s^{-1} are adsorbed by ethene molecules, the NaCl substrate is absorbing 2–10 times more 184.9 nm photons. The quantum efficiency based only on molecular ethene absorbance is $\Phi = 4 \pm 2$, but if we include contribution from the substrate, then $\Phi \leqslant 1$. Clearly the NaCl substrate is also an antenna of photon capture and its contribution to ethene photochemistry is significant.

Finally, we comment on the effects of the known structure of the ethene monolayer on the NaCl surface[61] which may be relevant to its photochemistry. As described elsewhere,[61] monolayer ethene on NaCl at 70 K has two molecules per unit cell in a roughly T-orientation with the molecular plane canted by *ca.* 25° from the surface. In this geometry we believe that both the ethylidene and vinylidene transition state structures are compatible. Of course, the photochemical experiment discussed here was executed at submonolayer coverages on vapour-deposited NaCl crystallites, while the monolayer determination was made on a homogeneous single crystal of NaCl. Comparison, however, should provide a useful first estimate of which excited path is feasible. The single crystal is essentially free of defect sites (*i.e.* colour centres) and the photochemistry should be affected.

Conclusion

As in our previous photochemical studies on the surface of NaCl crystallites,[10,11] we offer evidence that it is the substrate that is the principle antenna for photon capture and subsequent photochemistry. Energy stored in NaCl as triplet self trapped excitons (STEs) is transferred to the near resonant triplet of adsorbed ethene molecules. Triplet state ethene then transforms into ethylidene or vinylidene triplet intermediates than then eliminate H_2 molecules to produce acetylene. It appears that STEs in general may play an important role in alkali halide surface photochemistry.

The financial support of the National Science Foundation through NSF CHE95-05892 has made possible this research.

References

1 R. St. C. Smart and N. Sheppard, *J. Chem. Soc., Chem. Commun.*, 1961, 468.
2 R. St. C. Smart and N. Sheppard, *Proc. R. Soc. London, Ser. A*, 1971, **320**, 417.
3 R. St. C. Smart and N. Sheppard, *J. Chem. Soc., Faraday Trans. 2*, 1976, **72**, 707.
4 Y. A. Kozirovski and M. Folman, *J. Chem. Phys.*, 1964, **41**, 509.
5 J. H. De Boer, *Electron Emission and Adsorption Phenomena*, Cambridge University Press, Cambridge, 1935.
6 R. S. C. Smart, *Trans. Faraday Soc.*, 1971, **67**, 1183; R. S. C. Smart and P. J. Jennings, *Trans. Faraday Soc.*, 1971, **67**, 1193.
7 A. Zecchina and D. Scarano, *Surf. Sci.*, 1986, **166**, 347.
8 E. S. Kirkor, D. E. David and J. Michl, *J. Am. Chem. Soc.*, 1990, **112**, 139; E. S. Kirkor, V. M. Maloney and S. Michl, *J. Am. Chem. Soc.*, 1990, **112**, 148.
9 K. Leggett, J. C. Polanyi and P. A. Young, *J. Chem. Phys.*, 1990, **93**, 3645 and references therein.
10 S. K. Dunn and G. E. Ewing, *Faraday Discuss.*, 1993, **96/7**, 1.
11 S. K. Dunn and G. E. Ewing, *Chem. Phys.*, 1993, **177**, 571.
12 P. G. Wilkinson and R. S. Mulliken, *J. Chem. Phys.*, 1955, **23**, 1895.
13 A. J. Merer and R. S. Mulliken, *Chem. Rev.*, 1968, **69**, 639.
14 R. J. Sension and B. S. Hudson, *J. Chem. Phys.*, 1989, **90**, 1377.
15 M. B. Robin, *Higher Excited States of Polyatomic Molecules*, Academic Press, New York, 1985, vol. 3, p. 213 and references therein.
16 C. Petrongolo, R. J. Buenken and S. D. Peyerimhoff, *J. Chem. Phys.*, 1982, **76**, 3655.
17 R. S. Mulliken, *J. Chem. Phys.*, 1979, **71**, 556; 1977, **66**, 2448.
18 M. H. Palmer, A. J. Beveridge, I. C. Walker and T. Abuain, *Chem. Phys.*, 1986, **102**, 63.
19 R. J. Cvetanovic and A. B. Callear, *J. Chem. Phys.*, 1956, **24**, 873.
20 M. C. Sauer and L. M. Dorfman, *J. Chem. Phys.*, 1961, **35**, 497.
21 H. Okabe and J. R. McNesby, *J. Chem. Phys.*, 1962, **36**, 601.
22 E. Tschuikow-Roux, J. R. McNesby, W. M. Jackson and J. L. Faris, *J. Chem. Phys.*, 1967, **71**, 1531.
23 I. Tanaka and H. Hara, *Bull. Chem. Soc. Jpn.*, 1973, **46**, 3012; 1974, **47**, 1543.
24 A. Fahr and A. H. Laufer, *J. Photochem.*, 1984, **27**, 267; A. H. Laufer, *J. Photochem.*, 1986, **34**, 261.
25 B. A. Balko, J. Zhang and Y. T. Lee, *J. Chem. Phys.*, 1992, **97**, 935.
26 E. F. Cromwell, A. Stolow, M. J. Vrakking, Jr. and Y. T. Lee, *J. Chem. Phys.*, 1992, **97**, 4029.
27 S. Satyapal, G. W. Johnston, R. Bersohn and I. Oref, *J. Chem. Phys.*, 1990, **93**, 6398.
28 G. J. Collin, *Adv. Photochem.*, 1988, **14**, 135.
29 R. Gordon, Jr. and P. Ausloos, *J. Res. Natl. Bur. Stand.*, 1971, **75A**, 141.
30 S. Hirokami and R. J. Cvetanovic, *J. Phys. Chem.*, 1974, **78**, 1254.
31 K. Raghavachari, M. J. Frisch, J. A. Pople and P. V. R. Schleyer, *Chem. Phys. Lett.*, 1982, **85**, 145.
32 J. H. Jensen, K. Morokuma and M. S. Gordon, *J. Chem. Phys.*, 1994, **100**, 1981.
33 E. M. Evleth and A. Sevin, *J. Am. Chem. Soc.*, 1981, **103**, 7414.
34 O. Berg and G. E. Ewing, *J. Phys. Chem.*, 1991, **95**, 2908.
35 S. K. Dunn and G. E. Ewing, *J. Phys. Chem.*, 1993, **97**, 7993.
36 K. S. Song and R. T. Williams, *Self-Trapped Excitons*, Springer-Verlag, Berlin; in *Springer Ser. Solid-state Sci.*, 1993, **105**.
37 M. N. Kabler, *Phys. Rev. A*, 1964, **136**, A1296.
38 M. N. Kabler and D. A. Patterson, *Phys. Rev. Lett.*, 1967, **19**, 652.
39 V. N. Kadchenko and M. Elango, *Phys. Stat. Solidi A*, 1978, **46**, 315.
40 M. Ikeya and J. H. Crawford, Jr., *Phys. Lett. A*, 1973, **45**, 213.
41 R. G. Fuller, R. T. Williams and M. N. Kabler, *Phys. Rev. Lett.*, 1970, **25**, 446.
42 *Point Defects in Solids*, ed. J. H. Crawford and L. M. Slifkin, Plenum, New York, 1972, vol. 1.
43 A. Zecchina, D. Scarano and E. Garrone, *Surf. Sci.*, 1985, **160**, 482.
44 H. H. Richardson and G. E. Ewing, *Surf. Sci.*, 1987, **185**, 15.
45 G. E. Ewing, *Acc. Chem. Res.*, 1992, **25**, 292.
46 P. A. Cox and A. A. Williams, *Surf. Sci.*, 1986, **175**, L782.

47 S. G. Zvat and T. Y. Saks, *Sov. Phys. Solid State*, 1973, **14**, 2502.
48 T. Y. Saks and S. G. Zvat, *Sov. Phys. Solid State*, 1977, **19**, 1085.
49 A. P. Zhurakovskii, *Sov. Phys. Solid State*, 1981, **23**, 167.
50 S. P. McGlynn, T. Azumi and M. Kinoshita, *Molecular Spectroscopy of the Triplet State*, Prentice Hall, NJ, 1969.
51 J. B. Farmer, C. L. Gardner and C. A. McDowell, *J. Chem. Phys.*, 1961, **34**, 1058.
52 M. W. Schmidt and E. K. C. Lee, *J. Am. Chem. Soc.*, 1970, **92**, 3579.
53 S. Sato, R. J. Cvetanovic T. Terao and S. Hirokami, *Can. J. Chem.*, 1966, **44**, 2173.
54 S. Hirokami and S. Sato, *Can. J. Chem.*, 1967, **45**, 3181.
55 D. J. Dai and G. E. Ewing, *J. Chem. Phys.*, 1993, **98**, 5050.
56 S. Brunauer, I. H. Emmett and E. Teller, *J. Am. Chem. Soc.*, 1938, **60**, 309.
57 R. M. Stephenson, S. Malahowski, *Handbook of the Thermodynamics of Organic Compounds*, Elsevier, New York, 1987, p. 44.
58 O. Berg and G. E. Ewing, *Surf. Sci.*, 1989, **220**, 207.
59 L. M. Quattrocci and G. E. Ewing, *J. Chem. Phys.*, 1992, **96**, 4205.
60 S. K. Dunn and G. E. Ewing, *J. Phys. Chem.*, 1992, **96**, 5284.
61 K. R. Willian and E. G. Ewing, *J. Phys. Chem.*, 1995, **99**, 2186.
62 W. D. Shinzer, Doctoral Thesis, Indiana University, 1985.
63 J. Heidberg and P. Hoge, *J. Opt. Soc. Am. B, Opt. Phys.*, 1987, **4**, 242.
64 T. Shimanouchi, *Tables of Molecular Vibrational Frequencies*, American Chemical Society, New York, 1972, Part 1, NSRDS-NBS 6.
65 G. Zhao, M. J. Ospina and R. K. Khanna, *Spectrochim. Acta, Part A*, 1988, **44**, 27.
66 S. M. Blumenfeld, S. P. Reddy and H. C. Welsh, *Can. J. Phys.*, 1970, **48**, 513.
67 E. Rytter and D. M. Gruen, *Spectrochim. Acta., Part A*, 1979, **35**, 199.
68 R. K. Khanna, M. J. Ospina and G. Zhao, *Icrarus*, 1988, **73**, 527.
69 G. L. Bottyer and D. F. Eggers, *J. Chem. Phys.*, 1964, **40**, 2010.
70 M. Ito, J. Yokoyama and M. Suzuki, *Spectrochim. Acta., Part A*, 1970, **26**, 695.
71 B. Ma and H. F. Schaefer, *J. Am. Chem. Soc.*, 1994, **116**, 3539.
72 M. M. Gallo, T. P. Hamilton and H. F. Schaefer, *J. Am. Chem. Soc.*, 1990, **112**, 8714.
73 J. F. Stanton and J. Gauss, *J. Chem. Phys.*, 1994, **101**, 3001.
74 J. F. Stanton, C. M. Huang and P. G. Szalay, *J. Chem. Phys.*, 1994, **101**, 356.
75 R. A. Seburg and R. J. McMahon, *J. Am. Chem. Soc.*, 1992, **114**, 7183.
76 D. A. Modarelli and M. S. Platz, *J. Am. Chem. Soc.*, 1993, **115**, 470.
77 K. M. Ervin, J. Ho and W. C. Lineberger, *J. Chem. Phys.*, 1989, **91**, 5974.
78 R. A. Shepherd, T. J. Doyle and W. R. M. Graham, *J. Chem. Phys.*, 1988, **89**, 2738.
79 P. Dauber, M. Brith, E. Huler and A. Warshel, *Chem. Phys.*, 1975, **7**, 108.
80 E. Miron, B. Raz and J. Jortner, *Chem. Phys. Lett.*, 1970, **6**, 563.
81 T. Miyata and T. Tomiki, *J. Phys. Soc. Jpn.*, 1967, **22**, 209; 1968, **24**, 1286.
82 G. R. Elliot and G. E. Leroi, *J. Chem. Phys.*, 1973, **59**, 1217.
83 D. L. Pavia, G. M. Lampman and G. S. Kriz, Jr., *Introduction to Spectroscopy: A Guide for Students of Organic Chemistry*, Saunders College, Philadelphia, PA, 1979.
84 M. M. Gallo and H. F. Schaefer, *J. Phys. Chem.*, 1992, **96**, 1515.
85 K. M. Ervin, S. Gronert, S. E. Barlow, M. K. Gilles, A. G. Harrison, V. M. Bierbaum, C. H. DePuy, W. C. Lineberger and G. B. Ellison, *J. Am. Chem. Soc.*, 1990, **112**, 5750.
86 C. J. Wu and E. A. Carter, *J. Phys. Chem.*, 1991, **95**, 8352.

Paper 6/03906E; *Received* 4*th June*, 1996